Achieving enhanced gain in photorefractive polymers by eliminating electron contributions using large bias fields

C. M. Liebig,[1,2] **S. H. Buller,**[1] **P. P. Banerjee,**[3]
S. A. Basun,[1,2] **P.-A. Blanche,**[4] **J. Thomas,**[5] **C. W. Christenson,**[4]
N. Peyghambarian,[4] **and D. R. Evans**[1,*]

[1]*Air Force Research Laboratory, Materials and Manufacturing Directorate, Wright-Patterson Air Force Base, OH 45433, USA*
[2]*Azimuth Corporation, 4134 Linden Avenue, Suite 300, Dayton, OH 45432, USA*
[3]*University of Dayton, Department of ECE and Electro-Optics Program, Dayton, OH 45469, USA*
[4]*College of Optical Sciences, University of Arizona, Tucson, AZ 85721, USA*
[5]*NanoScience Technology Center and CREOL, College of Optics and Photonics, University of Central Florida, Orlando, FL 32816, USA*
[*]*corresponding author*

Abstract: Photorefractive polymers have been extensively studied for over two decades and have found applications in holographic displays and optical image processing. The complexity of these materials arises from multiple charge contributions, for example, leading to the formation of competing photorefractive gratings. It has been recently shown that in a photorefractive polymer at relatively moderate applied electric fields the primary charge carriers (holes) establish an initial grating, followed by a subsequent competing grating (electrons) resulting in a decreased two-beam coupling and diffraction efficiencies. In this paper, it is shown that with relatively large sustainable bias fields, the two-beam coupling efficiency is enhanced owing to a decreased electron contribution. These results also explain the cause of dielectric breakdown experienced under large bias fields. Our conclusions are supported by self-pumped transient two-beam coupling and photocurrent measurements as a function of applied bias fields at different wavelengths.

OCIS codes: (160.5320) Photorefractive materials; (160.5470) Polymers; (190.7070) Two-wave mixing.

References and links

1. S. Ducharme, J. C. Scott, R. J. Twieg, and W. E. Moerner, "Observation of the photorefractive effect in a polymer," Phys. Rev. E **66**, 1846–1849 (1991).
2. P. A. Blanche, A. Bablumian, R. Voorakaranam, C. Christenson, W. Lin, T. Gu, D. Flores, P. Wang, W. Y. Hsieh, M. Kathaperumal, B. Rachwal, O. Siddiqui, J. Thomas, R. A. Norwood, M. Yamamoto, and N. Peyghambarian, "Holographic three-dimensional telepresence using large-area photorefractive polymer," Nature **468**, 80–83 (2010).
3. A. Grunnet-Jepsen, C. L. Thompson, and W. E. Moerner, "Systematics of two-wave mixing in a photorefractive polymer," J. Opt. Soc. Am. B **15**, 905–913 (1998).
4. W. S. Kim, J. W. Lee, and J. K. Park, "Enhancement of the recording stability of a photorefractive polymer composite by the introduction of a trapping layer," Appl. Phys. Lett. **83**, 3045–3047 (2003).

#195572 - $15.00 USD Received 12 Aug 2013; revised 15 Nov 2013; accepted 19 Nov 2013; published 4 Dec 2013

5. C. W. Christenson, "Improving sensitivity of photorefractive polymer composites for holographic display applicaitons," Ph.D. thesis, The University of Arizona (2011).
6. P. P. Banerjee, S. H. Buller, C. M. Liebig, G. Cook, D. R. Evans, P. A. Blanche, C. W. Christenson, J. Thomas, and N. Peyghambarian, "Time dynamics of self-pumped reection gratings in a photorefractive polymer," J. Appl. Phys. **111**, 013108 (2012).
7. W. E. Moerner and S. M. Silence, "Polymeric photorefractive materials," Chem. Rev. **94**, 127–155 (1994).
8. M. Salvador, F. Gallego-Gomez, S. Köber, and K. Meerholz, "Bipolar charge transport in an organic photorefractive composite," Appl. Phys. Lett. **90**, 154102 (2007).
9. L. Wang, M. K. Ng, and L. Yu, "Photorefraction and complementary grating competition in bipolar transport molecular material," Phys. Rev. B **62**, 4973–4984 (2000).
10. M. C. Bashaw, T. P. Ma, R. C. Barker, S. Mroczkowski, and R. R. Dube, "Introduction, revelation, and evolution of complementarygratings in photorefractive bismuth silicon oxide," Phys. Rev. B **42**, 5641–5649 (1990).
11. D. R. Evans, S. A. Basun, M. A. Saleh, A. S. Allen, T. P. Pottenger, G. Cook, T. J. Bunning, and S. Guha, "Elimination of photorefractive grating writing instabilities in iron-doped lithium niobate," IEEE J. Quantum Electron. **38**, 1661–1665 (2002).
12. S. M. Silence, C. A. Walsh, J. C. Scott, T. J. Matray, R. J. Twieg, E. Hache, G. C. Bjorklund, and W. E. Moerner, "Subsecond grating growth in a photorefractive polymer," Opt. Lett. **17**, 1107–1109 (1992).
13. A. Veniaminov, T. Jahr, H. Sillescu, and E. Bartsch, "Length scale dependent probe diffusion in drying acrylate latex films," Macromolecules **35**, 808–819 (2002).
14. N. V. Kukhtarev, T. V. Kukhtareva, H. A. Abdeldayem, W. K. Witherow, B. G. Penn, D. O. Frazier, and A. V. Veniaminov, "Holographic recording in polymeric materials with diffusional amplification," Proc. SPIE **4459**, 29–38 (2001).
15. A. V. Veniaminov and E. Bartsch, "Diffusional enhancement of holograms: phenanthre-nequinone in polycarbonate," J. Opt. A Pure Appl. Opt. **4**, 387–392 (2002).
16. E. Bartsch, T. Jahr, T. Eckert, H. Sillescu, A. Veniaminov, "Scale dependent diffusion in latex films studied by photoinduced grating relaxation technique," Macromol. Symp. **191**, 151–166 (2003).
17. J. W. Oh, C. Lee, and N. Kim, "Infuence of chromophore content on the steady-state space charge formation of poly[methyl-3-(9-carbazolyl) propylsiloxane]-based polymeric photorefractive composites," J. Appl. Phys. **104**, 073709 (2008).

1. Introduction

Although photorefractive (PR) polymers have been successful in purely diffractive applications [1,2], they remain hindered by a suboptimal phase-shift between the local intensity pattern and the space-charge field in PR beam coupling applications [3]. According to the theory in [3], the suboptimal phase-shift is due to competition between the diffusion and the drift components of the space-charge field. In order to circumvent the suboptimal phase-shift and improve the PR response, one could theoretically apply larger applied electric fields. The higher applied fields allow the drift component to become the dominant contribution to the space-charge field and increases the PR phase-shift. A recent advancement in PR polymer devices is the application of thin inert buffer layers between the electrodes (ITO) and the PR polymer [4, 5]. The thin buffer layers enable the application of higher applied electric fields (> 70 V/μm) for longer periods of time by limiting electronic avalanche that causes excessive currents leading to dielectric breakdown in the polymer [4]. Although large applied fields can potentially be used to improve the amplitude and phase-shift of the index grating, it has also been observed that a mechanism present in state-of-the-art polymer systems may actually decrease the effectiveness of the space-charge field by the formation of competing (electrons) PR gratings created by the presence of oppositely charged carriers [6].

There are several possible sources for the opposite charge species forming competing gratings in PR polymers. In the organic photoconductors that are used, the primary charge carriers responsible for space-charge field formation are positively charged holes [7]. In the recent work of Banerjee *et al.* [6], it has been shown in a commonly used PR polymer, when the applied electric field is > 40 V/μm (using 532 nm light to record the grating), both holes and electrons become mobile and form competing space-charge fields, thereby reducing the PR gain. PR materials with competing gratings have been shown to decrease the diffraction efficiency

#195572 - $15.00 USD Received 12 Aug 2013; revised 15 Nov 2013; accepted 19 Nov 2013; published 4 Dec 2013

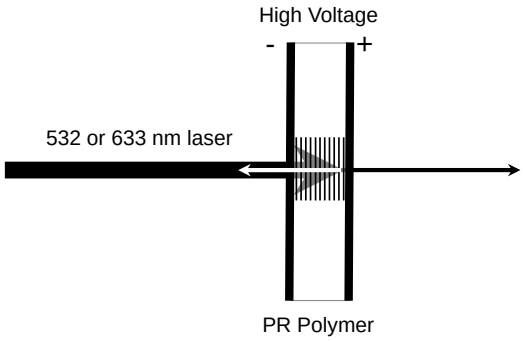

Fig. 1. PR polymer in self-pumped two-beam coupling geometry. The signal beam, represented by the small white arrow, is due to the counter-propagating Fresnel reflection of the incident pump beam. The small black arrow transmitted pump beam. The vertical black lines within the polymer represent the photorefractive index grating.

and two-beam coupling strength in both organic and inorganic materials, and have been modeled using the bipolar transport model [8–10]. Although the PR properties possessed by many of these polymer materials have shown potential, their applications have thus far been limited due to the competing gratings and the associated decrease in two-beam coupling strength and diffraction efficiency.

Competing space-charge fields are a detriment to PR polymer two-beam coupling and diffractive applications. If one of the contributing charge species can be modified (in terms of effective number density), then it may be possible that the effects of the competing grating could be negligible. In this paper our previous study in the state-of-the-art PR polymer 7-DCST:PVK:ECZ-BBP:C_{60} were extended to show when large sustainable bias fields are applied ($\approx$70 V/μm threshold field at 532 nm and $\approx$40V/μm threshold field at 633 nm), the detrimental effects of the competing electron gratings are eliminated, and the PR gain varies nonlinearly with the electric field. This material has been chosen as it is normally a single charge species polymer at lower applied fields, and it is the same material used in [6]. An improved fabrication process was used to reduce the occurrence of dielectric breakdown at high applied fields. All the polymers used in this study were tested to ensure their ability to survive the large potentials required to enhance the gain. Furthermore, we also explain how application of large electric fields ultimately cause dielectric breakdown.

2. Experimental conditions

To characterize the formation of the PR gratings in the polymer, for both the transient and steady states, self-pumped two-beam coupling was used. Self-pumped two-beam coupling is achieved in the reflection geometry, where the pump beam was incident upon the sample and the counter-propagating signal beam was produced by the Fresnel reflection from the back surface of the sample [11]. This geometry has the advantage of being more stable than our comparable two-beam coupling measurements in a transmission geometry due to the minimization of the phase fluctuations from external vibrations. Fig. 1 shows a schematic of the experimental setup. A linearly polarized CW frequency-doubled 532 nm Nd:YVO_4 laser (Coherent Inc.: Verdi 6) or a

#195572 - $15.00 USD Received 12 Aug 2013; revised 15 Nov 2013; accepted 19 Nov 2013; published 4 Dec 2013

633 nm helium neon laser (Melles Griot: 05-LHP-925), both attenuated to 10 mW output, was at normal incidence on the PR polymer cell. Note: the material studied in [6] is not labeled as containing a 7-DCST chromophore, it is indeed the same material as stated in this work. An electric field ranging from 20 V/μm to 70 V/μm was applied across the 100 μm thick sample in increments of 10 V/μm. The applied electric field (responsible for drift) is known to serve a twofold purpose: it drives the charge carriers via hopping through the photoconductor, and aligns the chromophore to increase the linear electro-optic effect. The PR grating formation was monitored by measuring the transmitted light through the sample with an optical power meter (Newport Corp.: Model 2832-C) as a function of time.

The time dynamics is monitored by subjecting the polymer to the laser light before the applied electric field, which allowed us to measure the chromophore reorientation in addition to the grating formation. Further information on this can be found in [6]. Absorption measurements were achieved using a CARY 5000. The steady-state photocurrent (using 532 nm and 633 nm incoherent light as an excitation source) was measured as a function of applied electric field (20 V/μm to 70 V/μm) using a Keithley 6514 electrometer.

3. Results and discussion

Figure 2 shows the time dynamics for the change in normalized transmission for both 532 nm and 633 nm as a result of two-beam coupling in the reflection geometry. It can be seen that the resulting measurements at 532 nm are similar to those previously measured by Banerjee *et al.* [6], although there are some differences in the behavior due to variations between samples. The resulting transmission of 532 nm light has been fit using a multi-exponential function for electric fields between 20 V/μm (small field) and 70 V/μm (large field). As previously reported [6], for relatively small applied fields (<40 V/μm at 532 nm) the decay can be adequately fit using a double exponential function with positive amplitudes for both exponential terms. These exponential terms correspond to the reorientation of the optical chromophore with the applied electric field and the formation of the PR grating formed by holes. For applied electric fields above a threshold ($\approx$40V/μm) a third component becomes measurable. This significant contribution is due to the competing grating formed by photo-excited electrons. This behavior has been thoroughly discussed by Banerjee *et al.* [6].

The temporal behavior of the transmission changes dramatically when applying fields at and above 70 V/μm (at 532 nm). Initially, there is a steep decrease of the transmission due to the chromophore reorientation and the formation of the hole grating, which is followed by a small increase in transmission due to the formation of the electron grating (i.e. the competing grating). At $t \approx 40$ s (for the case of 532 nm light) there is a further decrease in the transmission. This decrease has been repeatably measured in all of the polymer samples used for these measurements. For the samples used in [6], such a threshold was not obtainable. For all samples that have been measured, the threshold has varied between 70 V/μm and 75 V/μm, this can be attributed to variations between samples. This additional drop in transmission, i.e. increase in beam coupling efficiency, is not observed for the case of moderate fields when using 532 nm light.

An alternative way to view the enhanced gain, as shown in Fig. 3, is to plot the data in the same format as shown in Fig. 2 of [6]. The reduction in transmission in Fig. 3 is due to PR beam coupling, where the range of electric fields used was 60 to 75 V/μm in increments of 5 V/μm. The results in Fig. 3 only show the highest applied fields in order to reveal the detail of the transient data. Although it is not shown, a continuous decrease in the transmission with increasing applied fields was observed in a similar manner as shown in [6] Fig. 2; the main difference is the newly observed threshold field resulting in the enhanced PR gain. It is evident from the results shown in Fig. 2 and 3, that each individual sample can have a slightly

#195572 - $15.00 USD Received 12 Aug 2013; revised 15 Nov 2013; accepted 19 Nov 2013; published 4 Dec 2013

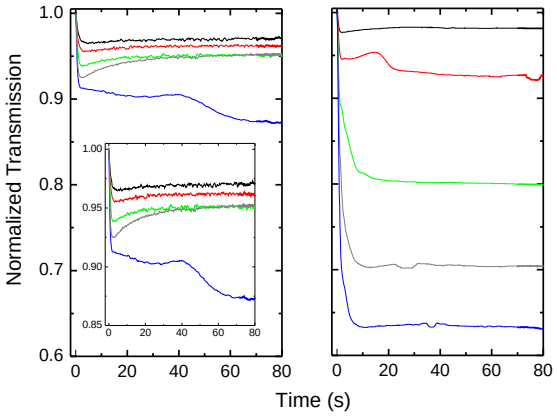

Fig. 2. Time dynamics of the grating formation using (left) 532 nm and (right) 633 nm light to record the gratings as a function of applied fields: in order from top to bottom - (black) 30 V/μm, (red) 40 V/μm, (green) 50 V/μm, (gray) 60 V/μm, and (blue) 70 V/μm. The scales on both graphs (left and right) are identical; the inset is the 532 nm data rescaled.

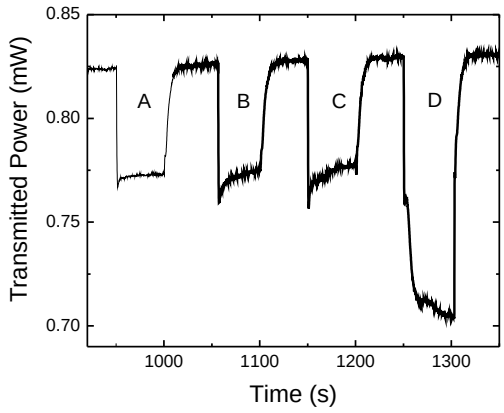

Fig. 3. Time response of the PR polymer gratings formed using 532 nm light with different bias voltages: A) 60 V/μm, B) 65 V/μm, C) 70 V/μm, and D) 75 V/μm. The region of gain enhancement is seen in plot D.

different threshold voltage. Over the series of samples used in this work, the gain enhancement was observed for field values between 70-75 V/μm. Unfortunately, the same sample could not be used for all measurements, as even though the issue of dielectric breakdown was improved, it was not eliminated. This figure in particular shows the dramatic nonlinear enhancement of the gain as a function of the electric field.

To further define the behavior of the PR polymers and to verify the results taken at 532 nm, the same measurements have been conducted in a different spectral region (633 nm) with less absorption, see Fig. 4 inset. The absorption coefficients at 532 nm and 633 nm are 162 cm^{-1}

#195572 - $15.00 USD Received 12 Aug 2013; revised 15 Nov 2013; accepted 19 Nov 2013; published 4 Dec 2013

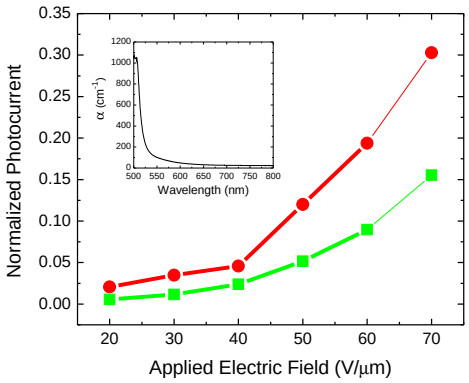

Fig. 4. The absorption compensated photocurrent as a function of applied electric field (20 V/μm to 70 V/μm): (red circles/lines) 633 nm and (green squares/lines) 532 nm. Inset: Absorption spectrum with zero field applied (uncorrected for reflection of glass windows and polymer material).

and 34 cm^{-1}, respectively. Incidentally, no significant changes were observed in the spectra as a function of applied field over the range of 0-80 V/μm. Figure 2 shows the time dynamics of the PR grating formation using a 633 nm laser to record the grating for applied fields between 20 V/μm and 70 V/μm. It can be seen that the overall grating formation behavior is similar to the measurement made using 532 nm, however, all essential features of the time dynamics for 633 nm occur at lower applied fields compared to 532 nm. The threshold applied electric field for the generation of the electron grating using 633 nm is noticeably less than the field required to generate the competing grating effect at 532 nm. Also, gain enhancement beyond the regime of competing gratings occurs at lower applied fields using 633 nm illumination ($\approx$40 V/μm compared to $\approx$70 V/μm observed using 532 nm); the enhanced gain is far more dramatic for the case of 633 nm than 532 nm. This enhanced gain and the associated reduction in the electric field threshold can be attributed to the increased photocurrent. One must also take into account the different absorption coefficients, when considering the photocurrent as a function of wavelength. The absorption compensated photocurrent is obtained by dividing the photocurrent by the absorption coefficient for the incident wavelength, and is shown in Fig. 4. The values of the absorption coefficients can be read from the inset in Fig. 4. It is clear that the absorption compensated photocurrent for 633 nm is a factor of two greater when compared to the photocurrent for 532 nm for the same applied field. Since the photocurrent is caused by the same charge carriers that are responsible for the grating formation, it is expected that the effects observed when using 633 nm recording light would occur at lower fields than when using 532 nm light.

A comparison of the two-beam coupling efficiency in terms of the change in optical density, ΔOD, for the steady state as a function of the applied electric field, is shown in Fig. 5. ΔOD is defined as $\log(T_0/T)$; T_0 and T are the transmission values before and after the formation of the PR grating, respectively. Fig. 5 shows the increase of the two-beam coupling efficiency due to the gain enhancement (beyond the regime of the electronic contribution to the PR grating), which is observed with large applied fields using 532 nm light and moderate applied fields using 633 nm light. The decrease in the applied field required for the enhanced ΔOD observed at 633 nm is explained by the increased absorption compensated photocurrent shown in Fig. 4.

#195572 - $15.00 USD Received 12 Aug 2013; revised 15 Nov 2013; accepted 19 Nov 2013; published 4 Dec 2013

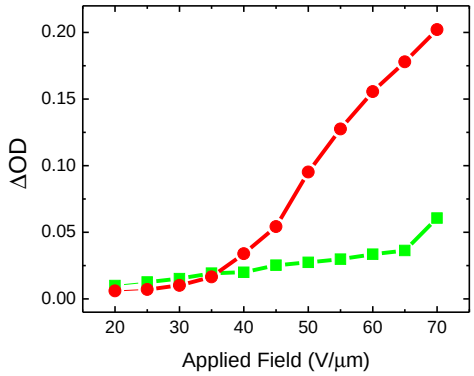

Fig. 5. Change in beam coupling efficiency (in terms of change in optical density, ΔOD) as a function of the applied electric field using 532 nm (Green Squares/Line) and 633 nm (Red Circles/Line) light. Note the threshold voltages for the onset of the nonlinear gain enhancement: ≈40 V/μm using 633 nm recording light and ≈70 V/μm using 532 nm recording light.

There are a few possible scenarios that can be proposed to explain the gain enhancement beyond the regime of competing gratings; these include contributions from either positive charges or positive ions. Based on previous interpretations of results [6, 9], the increased gain can be attributed to an additional charge species that is capable of forming a space-charge field present in the PR polymer, e.g. holes, electrons, ions. Hole and electron sources for the gratings are discussed in [6], and the presence of mobile ions resulting in ionic gratings has previously been proposed in [9, 12]. Regardless of the source, the two-beam coupling data shows that the gain enhancement complements the initial hole-formed grating, so electrons or negative ions contributions can be ruled out. If the buildup dynamics of the enhanced component of the grating formation is the same as the dynamics of the initial hole-formed grating, one can postulate that holes are involved; if the enhancement is significantly slower than the initial hole-formed grating response time, then positive ions would likely be the responsible source. To determine if the source of the gain enhancement is holes or positive ions, the data has been fit using a single exponential decay in Fig. 6 for reasons described in the following paragraphs. Exponential fits can be used to determine the relative amplitudes and formation times of individual components of a diffractive grating formed under many conditions; similar multi-exponential fitting has been used during the analysis of holographic recording with diffusional enhancement in polymeric materials [13–16].

The two-beam coupling data recorded using 633 nm light has been chosen for Fig. 6 since the gain enhancement occurs with a moderate applied electric field, allowing a greater range of fields to be explored that produce this gain. In Fig. 6(a), the grating dynamics at 633 nm include the initial reduction in transmission (photorefractive gain direction is opposite to the beam propagation direction), followed by the subsequent increase in transmission as a result of the competing electron-formed grating. Recall that this enhanced gain effect is rather strong at 40 V/μm when recording the grating with 633 nm, as opposed to the case of 532 nm where 40 V/μm is the threshold after which the competing electron grating becomes measurable. The contribution from chromophore reorientation has been neglected from the analysis of Fig. 6 since, as shown in [6], the associative time constant and the corresponding amplitude are both

#195572 - $15.00 USD Received 12 Aug 2013; revised 15 Nov 2013; accepted 19 Nov 2013; published 4 Dec 2013

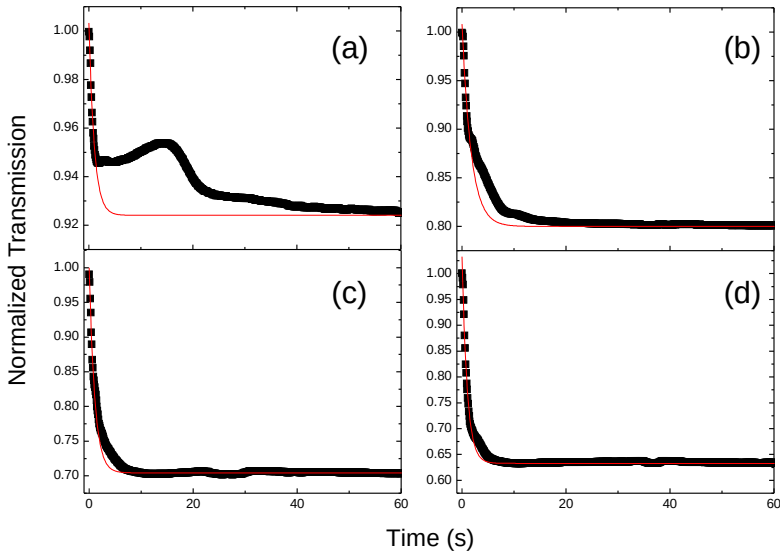

Fig. 6. Time dynamics of the grating formation using 633 nm light as a function of applied fields: (a) 40 V/μm, (b) 50 V/μm, (c) 60 V/μm, and (d) 70 V/μm. The data was fit with a single exponential, while ignoring the competing grating contribution. One time constant is responsible for the initial hole-formed grating and the long timescale nonlinear gain enhanced component.

comparatively small. Thus, a single exponential fit is purposely used in Figs. 6(a)–6(d) for bias fields ranging from 40 V/μm to 70 V/μm, thus ignoring the contributions from the electrons, this is done to determine if the same single exponential can fit the initial decay as well as the long-timescale enhanced gain region. The fits shown in Fig. 6 indicate the dynamics of the grating formation are indeed the same for the initial hole-formed grating and the enhanced gain region. Although Fig. 6 shows only the initial 60 s of the PR grating formation, the data was fit using the entire (120 s) data range. Had a multi-exponential term been required to fit both portions of the transmission curve (before and after competing grating formation), where one time constant is significantly longer than the other, positive ions could not be ruled out.

A possible mechanism for the gain enhancement, beyond the regime of competing electron-gratings, can be identified upon examining the trend of mobility shown in Fig. 5 in [6]. At higher fields the electron mobility is expected to exceed the hole mobility and it is surmised that due to this, the fast moving electrons are neither trapped nor recombine with the holes, and therefore no longer contribute to competing grating formation or reduction of the overall hole-formed grating. Hole-formed gratings again dominate in the two-beam coupling measurements as evidenced by above described single exponential fit for large electric fields, see Fig. 6(d). This being the case, the free electrons would contribute to the overall increased conductivity of the system, which explains why the polymers experience dielectric breakdown under large bias fields.

An alternate explanation in K space, for the observed effects is that at higher electric fields,

#195572 - $15.00 USD Received 12 Aug 2013; revised 15 Nov 2013; accepted 19 Nov 2013; published 4 Dec 2013

electron-hole recombination may not be possible due to momentum mismatch as a result of faster moving electrons, leading to predominantly hole-gratings. This momentum-concept can also be applied to the intermediate electric field regime. It can be postulated that a direct electron-hole recombination may occur due to momentum matching resulting in lower number of holes that can be trapped, thus reducing the beam coupling and diffraction efficiencies [17]. This would have the same detrimental effect on two-beam coupling and diffraction efficiencies as a competing grating, and both explanations require the presence of mobile electrons.

4. Conclusions

The presence of additional charge species has a considerable effect on the two-beam coupling strength of PR polymers. We have shown that when competing charge species are present, the two-beam coupling strength is decreased. This is because at moderately high applied fields electrons are mobile and become trapped, forming a competing space-charge field which reduces two-beam coupling gain and diffraction efficiency. For both 532 nm and 633 nm, nonlinear enhancement of the PR gain can be achieved by applying higher external fields. These larger fields allow for high electron mobilities (with respect to hole mobilities), which then do not contribute to competing grating formation. The mobile electrons contribute to increased conductivity, explaining why the polymers suffer dielectric breakdown under large bias fields. Due to reduced absorption at 633 nm, all observed transient effects occur at lower bias fields as compared to 532 nm.

#195572 - $15.00 USD Received 12 Aug 2013; revised 15 Nov 2013; accepted 19 Nov 2013; published 4 Dec 2013